Published online 20 February 2013

Nucleic Acids Research, 2013, Vol. 41, No. 7 ***4171–4184***
doi:10.1093/nar/gkt095

A novel nucleoid-associated protein specific to the actinobacteria

Julia P. Swiercz[1], Tamiza Nanji[2], Melanie Gloyd[2], Alba Guarné[2] and Marie A. Elliot[1,*]

[1]Department of Biology and Institute for Infectious Disease Research and [2]Department of Biochemistry and Biomedical Sciences, McMaster University, 1280 Main Street West, Hamilton, Ontario, Canada L8S 4K1

Received November 24, 2012; Revised January 24, 2013; Accepted January 25, 2013

ABSTRACT

Effective chromosome organization is central to the functioning of any cell. In bacteria, this organization is achieved through the concerted activity of multiple nucleoid-associated proteins. These proteins are not, however, universally conserved, and different groups of bacteria have distinct subsets that contribute to chromosome architecture. Here, we describe the characterization of a novel actinobacterial-specific protein in *Streptomyces coelicolor*. We show that sIHF (SCO1480) associates with the nucleoid and makes important contributions to chromosome condensation and chromosome segregation during *Streptomyces* sporulation. It also affects antibiotic production, suggesting an additional role in gene regulation. *In vitro,* sIHF binds DNA in a length-dependent but sequence-independent manner, without any obvious structural preferences. It does, however, impact the activity of topoisomerase, significantly altering DNA topology. The sIHF–DNA co-crystal structure reveals sIHF to be composed of two domains: a long N-terminal helix and a C-terminal helix-two turns-helix domain with two separate DNA interaction sites, suggesting a potential role in bridging DNA molecules.

INTRODUCTION

The bacterial chromosome serves as the blueprint for all cellular activity. This chromosomal blueprint is, however, subject to paradoxical organization: it must be extensively constrained and compacted so as to be effectively contained within a cell, and yet must be flexible enough to allow for not only transcription of the appropriate genes at any given time but also replication and segregation during cell growth and cell division. This dynamic behaviour is mediated, in part, by a group of proteins collectively termed the 'nucleoid-associated proteins'. These proteins bind DNA with varying degrees of specificity, and promote its compaction through DNA bending, bridging and wrapping (1). In addition to their structural function, many nucleoid-associated proteins also have a global impact on transcription, and their loss often results in pleiotropic phenotypic effects (1,2). Nucleoid-associated proteins have been most extensively studied in *Escherichia coli*, with IHF, HU and H-NS being among the best characterized. H-NS binds AT-rich DNA sequences, often within intergenic regions, and in such a way that the expression of flanking genes is repressed (3). It also oligomerizes with distantly bound H-NS molecules and effectively bridges disparate chromosomal DNA segments (4). Conversely, HU is a heterodimeric protein that binds DNA without any obvious sequence specificity and promotes DNA bending and wrapping (1,5). IHF is a structural homologue of the HU proteins. Like the HU proteins, IHF acts as a heterodimer, and its DNA binding leads to significant bending of the DNA, although unlike HU, it preferentially associates with specific DNA sequences (6).

While nucleoid-associated proteins are critical for chromosome organization in all bacteria, there is considerable diversity in the proteins that contribute to chromosome structure in different bacterial phyla. The actinobacteria, which include the filamentous *Streptomyces* and pathogenic *Mycobacterium,* for instance, encode HU-like proteins, but lack any obvious homologues to IHF or H-NS. Recent work in the mycobacteria has, however, revealed that these bacteria possess a functional equivalent to H-NS known as Lsr2 (7); there are two copies of Lsr2 encoded in most *Streptomyces* genomes sequenced to date. Lsr2 bears limited sequence and structural similarity to H-NS, but has analogous biochemical properties and is functionally interchangeable with H-NS in *E. coli* (7,8).

IHF had been investigated for its ability to stimulate phage DNA integration (hence its 'integration host factor' designation) prior to its characterization as a nucleoid-associated protein in *E. coli*. An equivalent activity has been observed for a protein in

*To whom correspondence should be addressed. Tel: +1 905 525 9140 (Ext 24225); Fax +1 905 522 6066; Email: melliot@mcmaster.ca

The authors wish it to be known that, in their opinion, the first two authors should be regarded as joint First Authors.

Mycobacterium tuberculosis and *Mycobacterium smegmatis*, whereby it facilitates bacteriophage DNA integration into the mycobacterial chromosome (9); this protein has subsequently been termed mIHF, for mycobacterial IHF. Like its *E. coli* namesake, mIHF is a small, heat-stable protein that promotes the integrative recombination of phage DNA with the chromosome by forming a stable intasomal complex with the phage integrase and *attP* DNA (9). Notably, *mIHF* is essential for *M. smegmatis* viability (10) and appears to be required for *M. tuberculosis* growth (11), suggesting that its function in the cell extends beyond phage DNA integration. Both IHF and mIHF accumulate to maximal levels during late exponential growth and entry into stationary phase (10,12,13). These proteins do not, however, share any obvious similarity at either a sequence or secondary structural level, they do not appear to bind similar DNA sequences (mIHF has no obvious sequence specificity while IHF exhibits preferred binding to a specific sequence), and IHF cannot function in place of mIHF (14), suggesting that their functional similarity may extend only to participation in phage DNA integration.

Probing the function of an essential protein like mIHF has its challenges, and thus we proposed to investigate the orthologous protein (SCO1480) in *Streptomyces coelicolor*. *Streptomyces* bacteria have an unusual life cycle, and because of this, some genes that are essential in the mycobacteria are not necessary to sustain growth of the streptomycetes. The streptomycetes and mycobacteria share a conserved genetic core, which encompasses most housekeeping and essential genes (15–17), and includes *SCO1480*/*mIHF*. They do, however, have very distinct life cycles. Mycobacteria are typically rod-shaped, grow by polar tip extension and divide by binary fission like many other bacteria (18). The streptomycetes also exhibit polarized tip growth, but instead of undergoing regular cell division, they grow filamentously, first establishing a branching vegetative mycelium and later raising aerial hyphae (19). These aerial hyphae undergo a defined maturation process that starts with coordinated septation which subdivides the hyphal filaments into pre-spore compartments and culminates with the differentiation of these compartments into chains of exospores (20). The streptomycetes are also distinguished by their prodigious secondary metabolic capabilities. Many of these metabolites have been co-opted for medical application and include a vast array of antibiotics (21). Secondary metabolism is intricately linked with the *Streptomyces* developmental program: aerial hyphae formation and antibiotic production are coordinately regulated, although the two processes are spatially segregated, with secondary metabolism occurring primarily in the vegetative hyphae (22). This unusual *Streptomyces* life cycle means that cell division and associated processes (e.g. chromosome segregation) are dispensable for viability, as cell division is only required during sporulation, while they would be essential in *Mycobacterium*.

Here, we probe the role of the mIHF orthologue, SCO1480—or 'sIHF' (23), in *S. coelicolor*, and provide evidence that these proteins constitute a new class of nucleoid-associated protein in the actinobacteria. We find that sIHF, unlike mIHF, is not essential for *S. coelicolor* viability, and instead is required for normal chromosome compaction, sporulation and secondary metabolism. We demonstrate that sIHF associates with the nucleoid *in vivo*, and apart from a preference for double-stranded over single-stranded DNA, it appears to bind DNA in a non-specific, but length-dependent manner. The crystal structure revealed that a monomer of sIHF associates with the minor groove of the DNA. sIHF interacts simultaneously with two DNA duplexes, and thus may have the capacity to bridge different DNA molecules. We have also found sIHF to impact the activity of topoisomerase *in vitro*, significantly affecting DNA topology. Taken together, these results suggest that sIHF and its orthologues are likely to function as novel actinobacterial-specific nucleoid-associated proteins.

MATERIALS AND METHODS

Bacterial strains and media

Streptomyces strains were grown on mannitol–soy flour (MS) agar, rich (glucose-containing) R2YE agar, or Difco nutrient agar (DNA), or in a 1:1 mixture of yeast extract–malt extract and tryptic soy broth (YEME-TSB) complex liquid medium (24). Strains were grown at 30°C for up to 10 days. *Escherichia coli* strains were grown at 37°C in liquid LB or SOB medium, or on LB agar plates, except for strains BW25113/pIJ790, which was grown at 30°C, and BT340, which was grown at either 30°C or 42°C. Strains and plasmids used in this study are listed in Table 1.

Creation of a *SCO1480*/*sIHF* knockout strain

An in-frame deletion of *SCO1480*/*sIHF* was generated using the ReDirect system described by Gust *et al.* (27). The *sIHF*-coding sequence (from start codon to stop codon) was initially replaced by an *oriT*-containing apramycin resistance cassette, before it was removed using Flp-mediated recombination, as described previously (27). Cassette removal was confirmed by testing the apramycin sensitivity of the mutant strain and further verified by PCR using primers SCO1480 ko 1/ko 2 (Supplementary Table S1). All subsequent phenotypic analyses were conducted using this in-frame deletion strain.

To complement the Δ*sIHF*-mutant phenotype, the *sIHF*-coding sequence was amplified, together with additional upstream (284 nt) and downstream (156 nt) sequences, using primers SCO1480 up and SCO1480 down (Supplementary Table S1). The PCR-amplified product was phosphorylated and cloned into the EcoRV site of the integrating vector pIJ82 (Table 1). The resulting construct was introduced into the Δ*sIHF*-mutant strain (E310a) via conjugation from *E. coli* strain ET12567/pUZ8002 (Table 1). pIJ82 alone was also introduced into both the mutant- and wild-type M600 strains as a control.

Table 1. Bacterial strains and plasmids

Streptomyces strains	Genotype	Reference
M600	SCP1− SCP2−	Chakraburtty and Bibb (25)
E310	M600 Δ*SCO1480(sIHF)::[aac(3)IV)-oriT]*	This work
E310a	M600 Δ*SCO1480(sIHF)::FRT*	This work
Escherichia coli strains	Use	Reference
DH5α	Plasmid construction and general subcloning	Invitrogen
ET12567/pUZ8002	Generation of methylation-free plasmid DNA	Paget *et al.* (26)
BW25113	Construction of cosmid-based knockouts	Gust *et al.* (27)
BL21 DE3 pLysS Rosetta	Protein overexpression	Novagen
BT340	DH5α carrying a 'FLP recombination' plasmid	Datsenko and Wanner (28)
Plasmids	Description and use	Reference
pIJ2925	General cloning vector	Janssen and Bibb (29)
pIJ773	Plasmid carrying the apramycin knockout cassette	Gust *et al.* (27)
pIJ790	Temperature sensitive plasmid carrying λ-RED genes	Gust *et al.* (27)
pIJ8660	Integrating plasmid vector carrying *eGFP*	Sun *et al.* (30)
pIJ82	Hygromycin-resistant integrating plasmid vector	Gift from H. Kieser
pET15b	6×His-tag protein fusion overexpression vector	Novagen
pMC153	pIJ8660 + *sIHF;* sIHF-eGFP localization	This work
pMC154	pIJ82 + *sIHF;* Δ*sIHF* complementation plasmid	This work
pMC155	pET15b + *sIHF;* overexpression of sIHF	This work
pMC141	pET15b + *srtA;* overexpression of SrtA	Duong *et al.* (31)
pET11a	Protein overexpression vector	Novagen
pAG8744	pET11a + *topA*; overexpression of TopA	This work
St9C5	Cosmid for *sIHF* knockout	Redenbach *et al.* (32)

Construction of a *sIHF–eGFP* translational fusion

The *sIHF*-coding sequence, along with 284 nt of upstream sequence, was amplified using Fuse 1 and Fuse 2 primers (Supplementary Table S1). These primers included BamHI and NdeI sites, respectively, within their 5′-ends to allow the resulting amplified product to be digested with the corresponding enzymes and cloned into the equivalent sites upstream of encoding an enhanced green fluorescent protein (*eGFP*) in pIJ8660 (Table 1). The Fuse 2 primer also included an extra 30 nt encoding a flexible linker peptide (LPGPELPGPE) to facilitate proper folding and functioning of the sIHF–eGFP fusion protein. This translational fusion was introduced into the Δ*sIHF*-mutant strain by conjugation (24) and was determined to function in place of the wild-type sIHF by testing for complementation of the mutant phenotype (antibiotic production, spore pigmentation and spore size).

Light, fluorescence and scanning electron microscopy

Samples for light and fluorescence microscopy were obtained by growing wild type, mutant and complementation strains along the underside of a sterile coverslip inserted into MS agar at a 45° angle. After 5 days, the coverslip was removed from the agar and adherent cells were stained with 4',6-diamidino-2-phenylindole (DAPI) diluted in a SlowFade solution (1:250; Invitrogen) and mounted onto a microscope slide. All images were obtained with a Leica DMI 6000 B wide-field deconvolution microscope using the Leica HCS Plan Apo oil immersion objective (magnification: ×100; numerical aperture: 1.4; Leica Microsystems, Wetzlar, Germany). Spore lengths, nucleoid areas and nucleoid fluorescence were all determined using ImageJ software (33). When visualizing eGFP, control strains (harbouring empty pIJ8660) were first examined to adjust fluorescence levels such that there was no detectable GFP signal, before imaging the experimental strains. Scanning electron microscopy was conducted on strains grown for 5 days on MS agar medium. Samples were prepared and visualized as described previously (34).

Antibiotic production assay

Equal numbers of wild type and mutant spores were used to inoculate 10 ml YEME-TSB liquid starter cultures that were grown for 2 days at 30°C. From these, an equivalent amount of biomass (~0.25 g) was used to inoculate 100 ml of YEME-TSB liquid medium. Levels of actinorhodin and undecylprodigiosin were measured every 24 h after inoculation for 6 days and were quantified using techniques described previously (35,36). Calcium-dependent antibiotic (CDA) bioassays were performed as outlined previously (24,37).

sIHF overexpression, purification, antibody generation and immunoblot analysis

sIHF was PCR amplified from chromosomal DNA using primers SCO1480 Nde and SCO1480 Bam (Supplementary Table S1). The resulting PCR product was introduced into SmaI-digested and dephosphorylated pIJ2925 (Table 1). *sIHF* was then excised by digestion with NdeI and BamHI and cloned into a similarly digested pET15b vector (Table 1). It was then sequenced and introduced into *E. coli* Rosetta cells (Table 1). Overexpression of 6×His-sIHF was achieved by growing cultures at 37°C to mid-exponential phase, before adding 1 mM isopropyl β-D-1-thiogalactopyranoside (IPTG) and growing them overnight at 26°C. Cells were resuspended in binding buffer (50 mM NaH_2PO_4, 300 mM NaCl and 10 mM imidazole, pH 8.0) containing 1 mg/ml lysozyme and one complete mini EDTA-free protease inhibitor pellet

(Roche), and incubated on ice for 30 min before being lysed by sonication. 6×His-sIHF was purified by passing the soluble protein extract over a Ni-NTA column (BioRad), washing with binding buffer supplemented with increasing concentrations of imidazole and eluting with 150 mM imidazole. The purified protein was then dialyzed into storage buffer (50 mM Tris, pH 7.5, 150 mM NaCl and 1 mM dithiothreitol [DTT]) and used for polyclonal antibody generation (Cedarlane Labs).

Protein samples were separated by sodium dodecyl sulphate (SDS)–polyacrylamide gel electrophoresis (PAGE) and were either visualized by staining with Coomassie Brilliant Blue to ensure equal sample loading, or were transferred to a polyvinylidene difluoride (PVDF) membrane. Membranes were blocked for 3 h at room temperature with Tris-buffered saline tween (TBST) 20, containing 10 mM Tris, pH 8.0, 100 mM NaCl and 0.05% Tween 20) containing 6% fat-free skim milk and subsequently incubated overnight at 4°C in TBST/6% skim milk containing crude polyclonal sIHF antibody (1:7000 dilution). The membrane was then washed three times with TBST, incubated for 30 min in TBST/6% skim milk containing goat anti-rabbit secondary antibody (1:3500 dilution) before again being washed three times with TBST.

Purification of untagged sIHF

The 6×His-sIHF was purified using a HiTrap Ni-chelating affinity column (GE Healthcare) equilibrated with 20 mM Tris, pH 8.0, 300 mM NaCl, 1.4 mM β-mercaptoethanol and 5% glycerol. Impurities were eliminated with a step gradient and 6×His-sIHF was eluted with 150 mM imidazole. Fractions containing 6×His-sIHF were pooled, diluted to adjust the salt concentration and loaded onto a 10/100 MonoS column (GE Healthcare) equilibrated with 20 mM Tris, pH 8.0, 100 mM NaCl, 1.4 mM β-mercaptoethanol and 5% glycerol. 6×His-sIHF was eluted using a linear salt gradient to 1 M NaCl. Fractions containing pure 6×His-sIHF were pooled, concentrated to 0.5 mg/ml and stored in storage buffer (20 mM Tris, pH 8.0, 150 mM NaCl, 1.4 mM β-mercaptoethanol and 5% glycerol). To cleave the histidine tag, 6×His-sIHF at 0.5 mg/ml was incubated with 0.03 units/μl of thrombin at room temperature for 60 min. The reaction was stopped with 1 mM benzamidine and sIHF was subsequently separated from the 6×His tag and thrombin over a 5/50 MonoS column (GE Healthcare).

Electrophoretic mobility shift assays

Electrophoretic mobility shift assays (EMSAs) were performed using 8–15% native polyacrylamide gels and [γ-^{32}P]dATP 5′-end-labelled probes. Increasing concentrations of sIHF (0–100 μM) were combined with 0.1 μM probe, 1 mg/ml bovine serum albumin (BSA) and binding buffer (10 mM Tris, pH 7.8, 5 mM $MgCl_2$, 60 mM KCl and 10% glycerol) and incubated at room temperature for 10 min and then on ice for 30 min prior to adding a glycerol-based loading dye. To test binding specificity, increasing concentrations of poly(dI-dC) (0–5 μg; Roche) were added together with 10 μM sIHF to the EMSA reactions described above. Gels were exposed to Kodak Biomax XAR film at room temperature for ~20 min before being developed. For probing sIHF binding to supercoiled (pUC19) versus linear (pUC19 digested with XbaI) DNA, 8 nM DNA was incubated with 0.08–17.3 μM sIHF in binding buffer as above, before reactions were separated on 1% TBE agarose gels and visualized by staining with ethidium bromide.

Cloning, protein overexpression and purification of TopA

The *S. coelicolor topA*-coding sequence was amplified from genomic DNA using primers topA1 and topA2 (Supplementary Table S1), and subcloned into pET11a using the NdeI and BamHI restriction sites to generate pAG8744. pAG8744 was transformed into BL21(DE3), grown to an OD_{600} of 0.7 and protein production was induced by adding 1 mM IPTG and incubating the culture for 3 h at 37°C. Cell pellets were resuspended in lysis buffer (20 mM Tris, pH 7.5, 25 mM KCl, 1.4 mM β-mercaptoethanol and 5% glycerol), lysed by sonication and cleared by centrifugation at 40 000g for 40 min. The supernatant was loaded onto a HiTrap SP HP column (GE Healthcare) equilibrated with lysis buffer. TopA was eluted using a linear gradient to 500 mM KCl. Fractions containing TopA were pooled together, concentrated to 3.5 mg/ml and stored at −80°C in 20 mM Tris, pH 7.5, 1.4 mM β-mercaptoethanol, 100 mM KCl and 25% glycerol.

Topoisomerase activity assays

The effect of sIHF on plasmids *in vivo* was assayed using *E. coli* Rosetta cells containing the 6×His-sIHF overexpression plasmid. Cells were grown to an OD_{600} of ~0.4, at which point expression of the sIHF fusion was induced using 1 mM IPTG. As a negative control, equivalent cultures were grown without IPTG induction. To test whether general protein overexpression led to changes in plasmid structure, the same experiment was conducted using pET15b containing *srtA* [pMC141; (31)], where *srtA* encodes an endopeptidase used to anchor proteins to the surface of Gram-positive cells. Plasmid DNA was extracted using the PureLink™ Quick Plasmid Miniprep Kit (Invitrogen) 8 h after induction, and the resulting DNA was separated by electrophoresis on a 0.8% agarose gel. Cell-free extracts for each culture (induced and uninduced) were also prepared and were separated on 12–18% polyacrylamide gels and stained with Coomassie Brilliant Blue to ensure both sIHF and SrtA were effectively expressed after 8 h of induction.

To assay the effect of sIHF or a negative control (lysozyme) on the activity of TopA, 5 μl of pUC19 (64 nM) was incubated with 1 μl of TopA (8 μg/ml), 0.6 μL of BSA (1 mg/ml), 8.4 μl of reaction buffer (50 mM Tris, pH 7.5, 50 mM KCl, 10 mM $MgCl_2$, 0.1 mM EDTA, 0.5 mM DTT and 0.06 mg/ml BSA) and 5 μl of either sIHF or lysozyme at 8.64, 17.28 or 34.56 μM (1:135, 1:270 and 1:540 [DNA:protein] molar excess, respectively). To ensure that neither sIHF nor lysozyme alone affected plasmid mobility, binding reactions were conducted as described above, only substituting storage buffer for TopA. Additional reactions at lower

DNA:sIHF molar excesses were conducted using sIHF at lower concentrations (1:17, 1:34, 1:68, 1:135, 1:270 and 1:540). Reactions were incubated at room temperature for 30 min and quenched with 5 µl of stop buffer (6% SDS, 30% glycerol, 10 mM EDTA and 0.25% bromophenol blue). All samples were resolved on 1% TAE-agarose gels, stained with ethidium bromide and visualized with UV light.

Protein crystallization

Complementary oligonucleotides 20 bp OH1 and 20 bp OH2 (Supplementary Table S1) were purchased from IDT, resuspended in deionized water to a final concentration of 6 mM, and annealed to form a 19-bp duplex (3 mM) with a single overhang on each duplex end. sIHF:DNA complexes (1:1 ratio) were prepared by mixing equal volumes of sIHF (3 mM) and DNA (3 mM), incubated for 10 min at room temperature and subsequently stored at 4°C. Crystals were grown at 4°C in 19% PEG 3350, 210 mM KSCN, 5% ethylene glycol, 100 mM HEPES, pH 7.6 and reached their final dimensions in ~2 weeks. Crystals were cryoprotected by dehydration against increasing concentrations of KCl (1–1.5 M) prior to flash freezing in liquid nitrogen. Seleno-methionine (SeMet)-labelled protein was produced in minimal medium supplemented with SeMet, as described elsewhere (38) and optimal crystals were grown in 18% PEG 3350, 210 mM KSCN, 5% ethylene glycol and 100 mM HEPES pH 7.6 from sIHF:DNA complexes prepared at 1:1.4 ratios.

Data collection and structure determination

A complete data set of SeMet-labelled sIHF:DNA was collected at X25 beam line in NSLS (Brookhaven National Laboratory, NY, USA). Data were indexed, processed and merged using HKL2000 (39) and the structure was phased by SAD using SOLVE (40). The initial model was refined by iterative cycles of manual building in Coot and refinement in phenix.refine (41,42). The final model encompasses residues 14–105 and has all residues within the most favoured regions in the Ramachandran plot (Supplementary Table S2).

RESULTS

sIHF is expressed throughout the *S. coelicolor* life cycle

As a first step in investigating the role of sIHF in *S. coelicolor*, we overexpressed and purified it as a 6×His-tagged fusion protein and generated α-sIHF polyclonal antibodies. We followed sIHF expression throughout the life cycle of *S. coelicolor* (over a 4-day time course), during growth on either MS (poor carbon source) or R2YE (rich) agar media. Immunoblotting revealed that the cytoplasmic sIHF protein was present throughout development on MS agar medium, with levels gradually decreasing as development proceeded (Figure 1). On R2YE, levels were roughly equivalent at all times apart from 72 h, where there was a modest dip in expression (Figure 1). This is in contrast to mIHF and IHF, which typically accumulate later in growth (10,12,13). To ensure that we were examining equivalent amounts of protein, we separated cell-free extract samples on an SDS–polyacrylamide gel and stained the fractionated proteins with Coomassie Brilliant Blue (Supplementary Figure S1).

Loss of *sIHF* impacts development and antibiotic production

Despite the essential nature of the sIHF orthologue in *Mycobacterium* (mIHF), it turned out to be remarkably straightforward to delete *sIHF* in *S. coelicolor*. One of the most immediately striking phenotypes of the *sIHF* knockout mutant was its aberrant production of pigmented antibiotics when grown either on solid agar (Figure 2A) or in liquid culture (Figure 2B). During growth on MS agar medium, there was no obvious actinorhodin (blue) production, and little undecylprodigiosin (red) production relative to its wild-type parental strain; however, on R2YE, the mutant exhibited enhanced actinorhodin production (Figure 2A). During growth in a complex liquid medium (YEME-TSB), production of both pigmented antibiotics was significantly delayed and dramatically reduced for the Δ*sIHF*-mutant strain compared with the wild type (Figure 2B). We also tested CDA production using a plate-based bioassay and found that after 48 h of growth, the mutant failed to produce any CDA, while the wild-type strain produced levels that effectively inhibited growth of the indicator strain (*Staphylococcus aureus*; Figure 2C). The mutant phenotypes could be restored to near wild-type levels by re-introducing the wild-type *sIHF* gene under the control of its own promoter, on the integrating plasmid vector pIJ82 (Figure 2A and C).

We also found the Δ*sIHF* mutant grew more slowly than the wild type, and exhibited sporulation defects, including reduced levels of sporulation, as well as aberrant spore septum placement and consequently greater heterogeneity in spore size (Supplementary Figure S2), confirming previous observations reported by Yang *et al.* (23).

Aberrant chromosome compaction and segregation during sporulation of an *sIHF*-mutant strain

During vegetative and aerial hyphal growth, chromosomes appear diffuse, and it is only during sporulation—the reproductive phase of *Streptomyces* development—that the chromosomes are compacted and segregated into the future spore compartments. Given the abnormal spores resulting from the deletion of *sIHF*, we were interested in determining whether *sIHF*-mutant strains also exhibited defects in chromosome organization during sporulation.

We first compared the overall DNA content of spores ($n > 1000$) and found that anucleate spores were far more common in the Δ*sIHF*-mutant strain (8.6%) than in the wild-type strain (0.3%). Introducing a wild-type copy of *sIHF* into the Δ*sIHF* mutant reduced the level of anucleate cells to ~2%. When comparing the nucleoids of wild type and mutant spores, we also observed differences in their levels of chromosome compaction, with

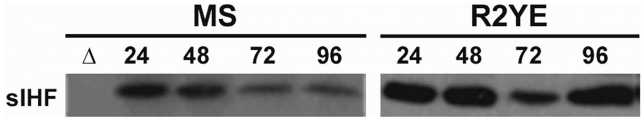

Figure 1. Western blot analysis of sIHF production. sIHF production is shown in wild-type *S. coelicolor* when grown on MS or R2YE media. Samples were taken at the indicated times (hours). The Δ*sIHF*-mutant strain (Δ) was used as a negative control.

mutant spore DNA seeming more diffuse than those of the wild type, and in some instances adopting a 'bilobed' configuration (Figure 3A), although we did occasionally observe this for wild-type chromosomes as well (Figure 3C). We quantified the nucleoid area for both wild-type and Δ*sIHF*-mutant spores and found wild-type nucleoids were indeed more compact than those of the mutant, with the average size being 0.33 μm^2, versus 0.60 μm^2 for the Δ*sIHF* mutant (Figure 3B). Similar to what was observed for spore size, nucleoid area also showed a different distribution for the two strains, with >90% of wild-type nucleoids occupying an area of between 0.18 and 0.57 μm^2, while the same proportion of mutant nucleoids exhibited a range of 0.31–0.98 μm^2. Complementation with a wild-type copy of *sIHF* restored wild-type-like chromosome compaction in the Δ*sIHF* mutant (Figure 3B). We considered the possibility that the more diffuse nucleoids observed in the Δ*sIHF* mutant might reflect increased DNA content, but we failed to detect any significant differences in the DNA content of wild type and mutant spores ($n > 1000$), as determined by measuring DAPI fluorescence intensity per spore.

Given the effect that *sIHF* deletion had on chromosome architecture in sporulating cells, we also probed the intracellular localization of sIHF using an sIHF–eGFP fusion. This construct effectively complemented the mutant phenotype (restoring antibiotic production on MS agar and wild-type spore size to the mutant; Supplementary Figure S3), indicating that the fusion protein was functional. Using fluorescence microscopy, we found sIHF–eGFP co-localized with the condensed nucleoid during sporulation (Figure 3C). To ensure that the pattern we observed reflected nucleoid association and not simply cytoplasmic distribution, we compared the fluorescence pattern observed for the *sIHF–eGFP*-containing strain, with that of wild-type spores expressing eGFP under the control of the *chpH* promoter, which is expressed at high levels during sporulation (43). In this instance, the eGFP pattern was more diffuse than that of sIHF–eGFP and occupied the entire spore compartment (Figure 3C). Considering the nucleoid localization of sIHF, together with the sporulation and chromosome segregation/compaction defects observed for the *sIHF*-mutant strain, this suggests that sIHF may play a key role in coupling changes in chromosome architecture with appropriate cell division during *Streptomyces* sporulation.

sIHF interacts non-specifically with double-stranded DNA

Recent studies have suggested a role for sIHF as a transcriptional regulator (23,44), and previous work on

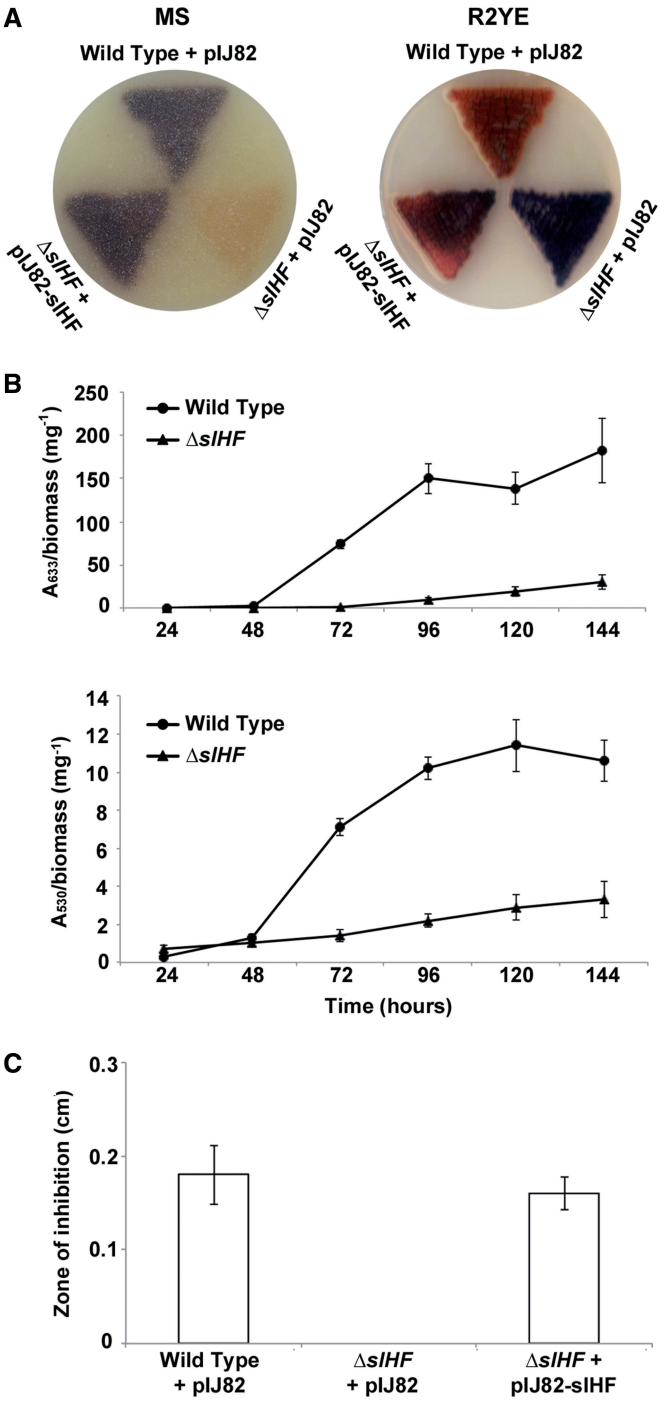

Figure 2. *Streptomyces coelicolor* antibiotic production in the absence of *sIHF*. (**A**) Plasmid-containing wild type (M600) and Δ*sIHF* in-frame deletion strains, as well as the complemented Δ*sIHF*-mutant strain, were grown on MS (left) and R2YE (right) agar media for 5 and 4 days, respectively. Images were taken from the underside of each plate to effectively display antibiotic production. (**B**) Actinorhodin (top) and undecylprodigiosin (bottom) production by wild-type and Δ*sIHF*-mutant strains in complex liquid YEME-TSB medium over a 6-day time course. (**C**) CDA production assay by plasmid-containing wild-type and Δ*sIHF*-mutant strains, along with the complemented Δ*sIHF*-mutant strain.

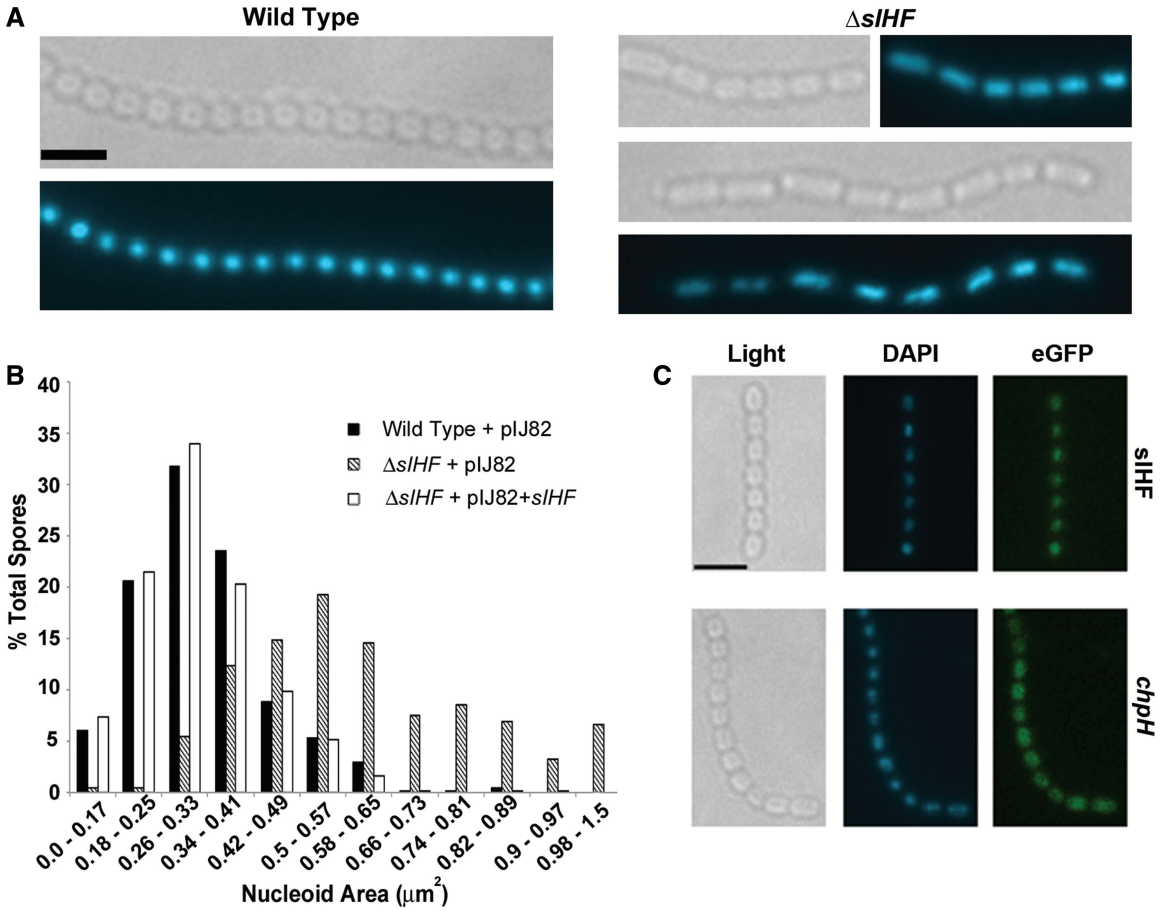

Figure 3. sIHF localization within spore compartments relative to chromosomal DNA. (**A**) Light and DAPI fluorescence images of wild-type (left panels) and Δ*sIHF*-mutant (right panels) strains. Each image set depicts the same spore chain. The scale bar represents 2.6 μm. (**B**) Comparison of nucleoid areas for wild type, mutant and complemented strains, with calculated areas rounded to the nearest 0.01 μm^2. 500–600 spores were examined for each strain. (**C**) Light and fluorescence microscopy (DAPI and GFP) images of wild-type spores expressing an sIHF-eGFP translational fusion (top panels) or P_{chpH}-*eGFP* transcriptional fusion (bottom panels). The DAPI panel shows chromosomal DNA localization, while the eGFP panel shows the localization of eGFP when fused to either sIHF or the *chpH* promoter. Scale bar represents 3.2 μm.

the mycobacterial orthologue mIHF showed it to associate indiscriminately with double-stranded DNA (9). We set out to systematically assess the DNA-binding specificity of sIHF using EMSAs. We started by incubating purified protein with a short DNA duplex (19 bp) and found the probe was shifted in a concentration-dependent manner, although a clearly defined shift was not observed (Figure 4A). To explore the length dependence of sIHF binding, we next tested two double-stranded DNA probes that were approximately two and three times the length of the 19 bp probe (43 and 60 bp, respectively); these probes corresponded to the coding sequence of a gene (*SCO4676*) whose product has no obvious role in the development or antibiotic production of *S. coelicolor* under the conditions examined here (Hindra and Elliot,M.A., unpublished data). In each case, a complete shift of all labelled probe was observed with 10 μM sIHF, giving a discrete complex at the top of the gel (Figure 4A and Supplementary Figure S4). When we extended the length of the labelled probe to 407 bp, sIHF binding was further enhanced: >50% of the probe was shifted in the presence of 0.5 μM sIHF, a complete shift was observed with 3 μM sIHF and 10 μM sIHF led to a discrete shifted complex that was unaffected by further protein addition (Figure 4B). These results imply that effective complex formation between sIHF and DNA is length dependent, and that sIHF binding may be cooperative.

We next probed the binding specificity of sIHF, conducting competition assays using increasing concentrations of poly(dI-dC), together with the labelled 60 (Supplementary Figure S4) and 407 bp probes (Figure 4B). We found that as little as 0.3 μg of poly(dI-dC) was sufficient to eliminate all binding to the 60 bp probe, while 2.5 μg of poly(dI-dC) abolished binding to the 407 bp probe, confirming that there was little specificity associated with sIHF–DNA binding. This is notable, when considering that 1 μg of poly(dI-dC) (three times the concentration needed to eliminate all binding to the 60 bp probe) is frequently used as an internal competitor in DNA-binding reactions (e.g. [37,45]). Interestingly, the amount of poly(dI-dC) required to effectively compete for sIHF binding was proportional to the length of the labelled probe: the 407 bp probe is approximately seven times longer than the 60 bp probe, and required eight

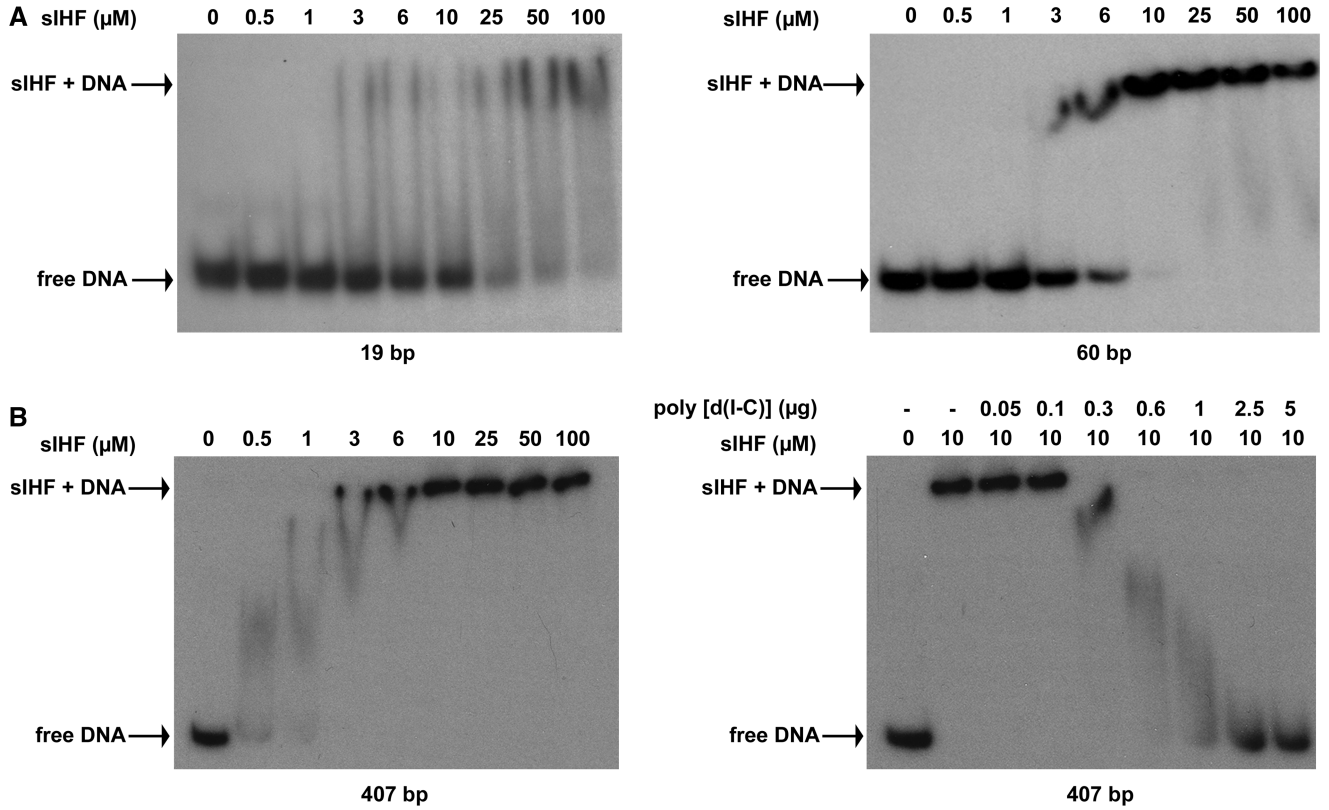

Figure 4. DNA binding by sIHF. (**A**) EMSAs showing sIHF binding to probes of increasing length. Increasing concentrations of sIHF were added to the indicated DNA probes. Panels represent the binding of sIHF to a 19-bp DNA probe (left) and a 60-bp DNA probe (right). (**B**) EMSAs showing the binding affinity of sIHF to a 407-bp DNA probe. The left panel shows sIHF–DNA complex formation in the presence of increasing concentrations of sIHF. The right panel shows the effect of increasing poly(dI-dC) concentrations on sIHF–probe complexes.

times the amount of poly(dI-dC) for full competition. These results all support a model in which sIHF binds DNA without any obvious sequence specificity, in a concentration and length-dependent manner.

sIHF specificity in binding to DNA with distinct conformations

Having determined that sIHF was required for normal chromosome segregation and compaction through our genetic analyses, and having shown that it was a promiscuous binding protein *in vitro*, we were interested in trying to understand how its DNA-binding activity impacted chromosome dynamics in the cell. Many nucleoid-associated proteins bind DNA without any defined sequence specificity, but preferentially associate with defined DNA structures. For example, in *E. coli,* H-NS binds curved DNA with highest affinity (46,47), while HU has strong affinity for distorted (e.g. gapped) DNA configurations (48). We therefore set out to determine whether sIHF had increased affinity for DNA having different structures, or whether it influenced DNA structure upon binding. We began by comparing the affinity of sIHF for linear DNA versus curved and gapped sequences, but found no reproducible difference in sIHF affinity for any of these different DNA conformations (data not shown). We also compared the relative affinity of sIHF for linear versus supercoiled DNA, and again, we observed equivalent binding to both DNA forms (data not shown). We went on to investigate the ability of sIHF to associate with single-stranded DNA, as this has been shown to be a substrate for several nucleoid-associated proteins in other bacteria, including the SMC protein in *Bacillus subtilis* (49). We tested binding using labelled probes corresponding to either strand of the 60 bp probe tested above. These single-stranded sequences did not have any significant hairpin potential or extended self-complementarity. While we observed concentration-dependent interactions with the single-stranded probes, complete shifting of the probe was never observed, even in the presence of 100 μM sIHF (Supplementary Figure S4). This is in stark contrast to the equivalent double-stranded sequence, where 10 μM sIHF was sufficient to shift all probe (Figure 4A), indicating that sIHF has a strong preference for double-stranded DNA, relative to single stranded. To determine whether sIHF influenced DNA structure upon binding, as has been observed for nucleoid-associated proteins such as IHF (50,51), we tested the ability of sIHF to bend DNA upon binding using FRET analysis, but did not detect any obvious changes in fluorescence when comparing samples incubated in the presence or absence of sIHF (data not shown). Collectively, these results suggest that, apart from preferentially binding double-stranded DNA, sIHF does not discriminate between different DNA configurations, at least *in vitro*.

sIHF enhances topoisomerase activity

In an attempt to further probe the means by which sIHF impacts chromosome organization, we wanted to assess its effect on enzymes that influence DNA supercoiling and chromosome compaction. As a first step, we took advantage of our sIHF overexpression construct, and introduced this construct into *E. coli*, and compared the topology of plasmids isolated following sIHF overexpression/induction relative with those isolated from an uninduced strain. We consistently observed different plasmid topologies for the sIHF overexpressing strain relative to its uninduced control (Figure 5A). To ensure that the addition of IPTG did not impact plasmid conformation, we also examined plasmids isolated from strains expressing an unrelated protein (SrtA) from the same plasmid, and we did not see any differences in plasmid configuration in the induced versus uninduced strain (Figure 5A). We confirmed in each case, that expression of sIHF and SrtA had been effectively induced, and that these proteins were present at much higher levels than in the uninduced cultures (Supplementary Figure S5).

These results suggested that sIHF might influence DNA supercoiling. To further investigate this possibility, we conducted an *in vitro* assay aimed at assessing the effect of sIHF on the activity of TopA—the sole type I topoisomerase encoded by *S. coelicolor*. Using purified TopA, we followed its activity in the presence and absence of sIHF, using supercoiled *E. coli* plasmid DNA as a substrate. We found sIHF had a profound effect on plasmid topology, appearing to counteract the relaxation activity of TopA (Figure 5B). Importantly, sIHF alone did not affect plasmid supercoiling and relaxation, nor was the sIHF concentration used for these reactions sufficient to shift the plasmid DNA (Figure 5B and C). To confirm that the observed effects were specific to sIHF, we repeated the experiment, substituting lysozyme (another small protein) for sIHF, and did not observe any change in plasmid topology (Figure 5C). These findings imply that sIHF makes a significant contribution to DNA conformation and topology in a topoisomerase-dependent manner.

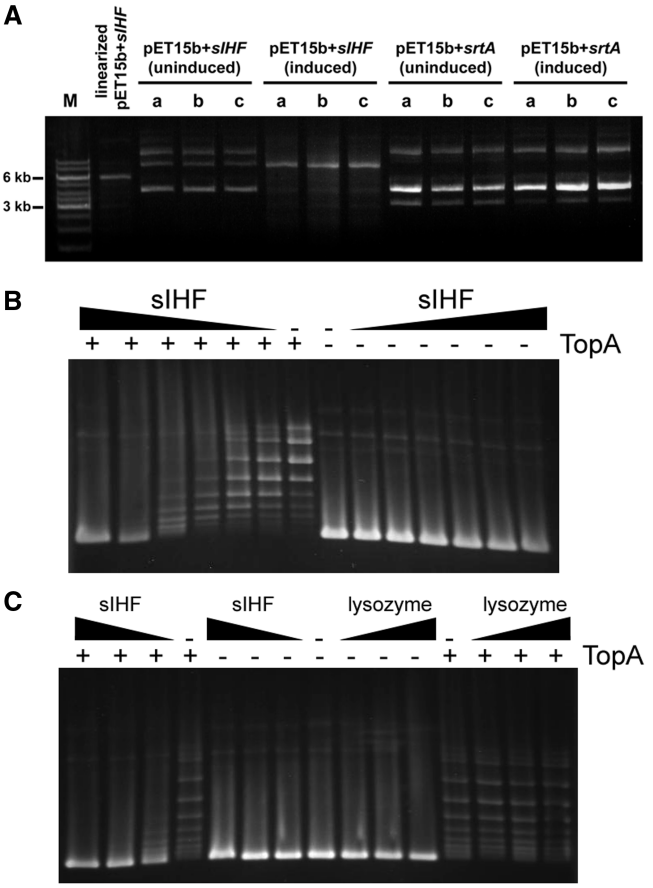

Figure 5. sIHF alters plasmid DNA supercoiling. (**A**) pET15b containing either *sIHF* (left) or *srtA* (right), isolated from *E. coli*. IPTG was added to three independent cultures (a, b and c) to induce overexpression of *sIHF* and *srtA*, while three others were grown without induction prior to plasmid harvest. For size comparison, a marker (M) was run alongside linearized (NdeI digested) pET15b+*sIHF*. (**B**) The minimal amount of sIHF able to affect TopA activity was assayed by incubating supercoiled pUC19 plasmid DNA with serially diluted sIHF (1:540 to 1:17 [pUC19:sIHF] molar excess) in the presence/absence of TopA. (**C**) Supercoiled pUC19 plasmid DNA was incubated alone, or together with increasing concentrations of either sIHF or lysozyme (at 1:135, 1:270 and 1:540 [DNA:protein] molar excess), in the presence/absence of *S. coelicolor* TopA (8 μg/ml) as indicated.

Structure of sIHF bound to DNA

The *in vitro* and *in vivo* behaviour of sIHF determined to this point were not consistent with that of any known nucleoid-associated protein, and while the activity of the sIHF orthologue in the mycobacteria (mIHF) in promoting phage DNA integration mirrored that of IHF in *E. coli*, we suspected that neither sIHF nor mIHF were structural or functional homologues of IHF. We therefore sought to determine the crystal structure of sIHF in complex with the 19-bp DNA duplex used for our initial EMSA experiments (Figure 4A). Crystals of sIHF bound to DNA diffracted to 2.7 Å resolution and, of the 107 amino acids of sIHF, we were able to model residues 14–103 in the experimental electron density maps (Supplementary Table S2). The sIHF structure is composed of a long and protruding N-terminal α-helix (α1) followed by four shorter α-helices that define the core of the protein (Figure 6A). The arrangement of the helical core resembles that of a small domain found in the structures of type IIb topoisomerases (specifically topoisomerase VI), the endonuclease VIII family of base excision repair enzymes and the ribosomal protein S13 (52–55) (Figure 6D–F). This domain includes a characteristic helix-two turns-helix (H2TH) motif, spanning α3 to α4 in sIHF (Figure 6C). While the specific function of the H2TH domain in these proteins is unknown, the structures of the small S13 ribosome subunit and endonuclease VIII bound to DNA reveal that the two turns connecting the helices of the motif may enhance binding to nucleic acids in an unspecific manner (Figure 6E and F).

sIHF binds DNA as a monomer, and although a 19-bp DNA duplex was used to assemble the sIHF–DNA complex, only eight nucleotides fit in the asymmetric unit. Adjacent DNA molecules stack end-to-end, forming a pseudo-continuous duplex that runs parallel

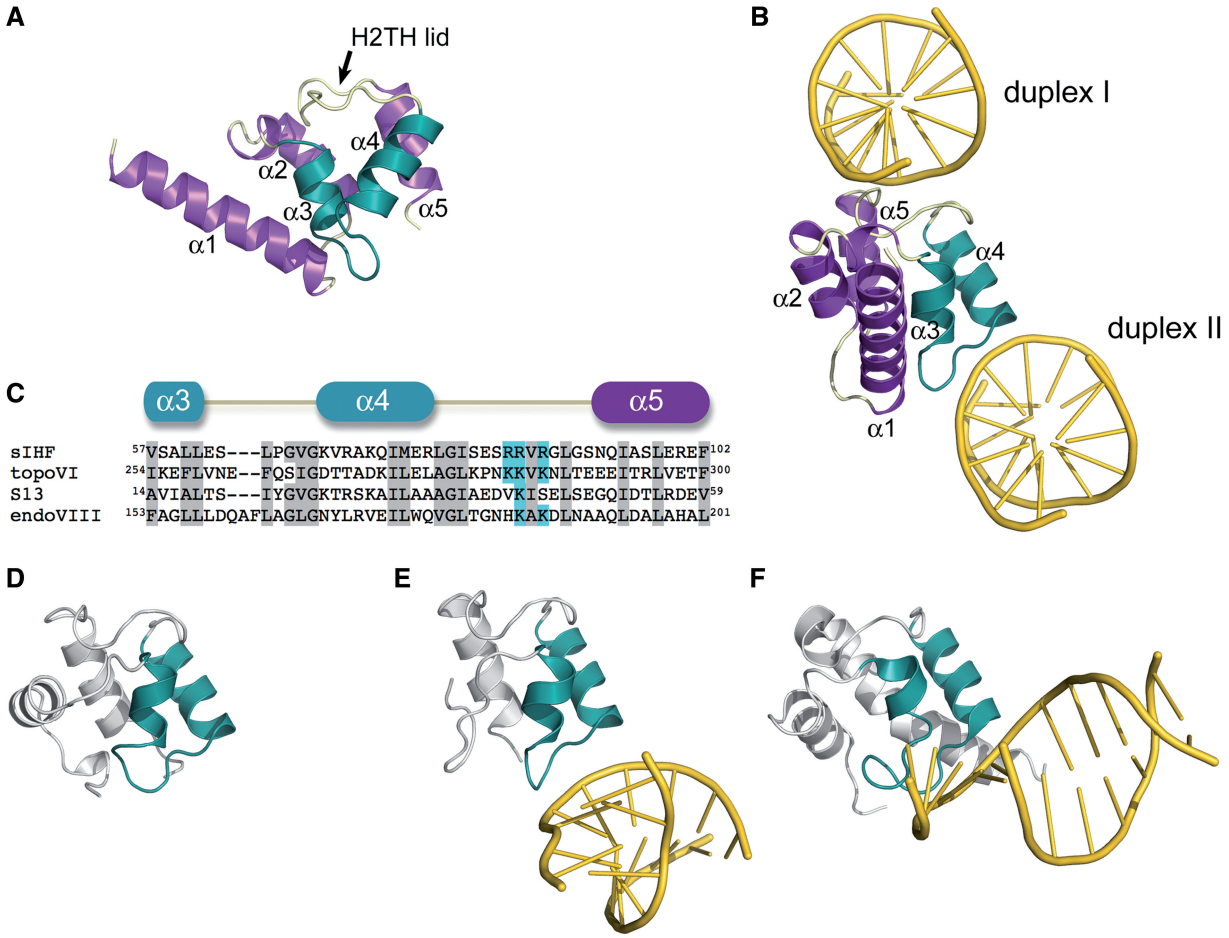

Figure 6. Structure of sIHF. (**A**) Ribbon diagram of sIHF with helices shown in purple, loops in cream and the H2TH motif coloured in teal. (**B**) Interaction of sIHF with neighbouring DNA molecules (shown in yellow). The view is rotated 90° with respect to the view in panel (A) and the two neighbouring DNA duplexes are labelled for reference. (**C**) Sequence alignment of the hydrophobic core of sIHF, the H2TH domain of topoisomerase VI, the N-terminal domain of the ribosomal protein S13 and the H2TH domain of endonuclease VIII. Conserved hydrophobic residues are shadowed in grey and conserved charged residues in the H2TH lid are highlighted in cyan. (**D**) Ribbon diagram of the H2TH domain of topoisomerase VI (residues Lys230-Phe306, PDB ID 1MU5). (**E**) Ribbon diagram of residues Ala1-Phe62 from the ribosomal protein S13 (PDB ID 2GY9). (**F**) Ribbon diagram of the H2TH domain of endonuclease VIII (residues Pro132-Gln214, PDB ID 1K3W).

to one axis of the unit cell. Given its lack of binding specificity, sIHF has the potential to associate with any sequence within these long duplexes, and it appears that the crystal captured an average distribution of sIHF over the entire length of the duplex DNA. Accordingly, the phosphate backbone of the DNA duplex was clearly defined in the experimental electron density maps (Figure 7), but the nucleotide sequence of the DNA duplex bound by sIHF could not be assigned, reinforcing the idea that the 8 bp in the asymmetric unit represent an average of different bases. Since we used a GC-rich sequence to prepare the duplex DNA, we modelled the base moieties as guanines or cytosines based on the relative size of the electron density.

sIHF contacts two of these pseudo-continuous DNA duplexes via distinct regions (Figures 6B and 7). The protein associates with duplex I through the 11-residue 'lid' that connects helices α4 and α5. This lid appears to have a dual function, serving to both conceal the hydrophobic core of the protein (Figure 6A) and provide a flat surface rich in positively charged residues (Figure 6C) that cradles the phosphate backbone of one of the DNA strands of duplex I. One of the duplex phosphate moieties further stabilizes this interaction by neutralizing the dipole moment of helix α5 (Figure 7A). Interestingly, this lid adopts a nearly identical conformation in the structures of topoisomerase VI and ribosomal protein S13 (Figure 6D–E). In the monomer and dimer structures of topoisomerase VI, the lid is exposed to the solvent and is more accessible than the H2TH motif in sIHF; however, it is not possible to infer a role for this feature in DNA binding by topoisomerase VI, as DNA is not present in that structure (52).

The interface between sIHF and duplex II is less extensive than that of sIHF and duplex I, involving only the second turn of the H2TH motif and one phosphate moiety neutralizing the dipole moment of helix α4 (Figure 7B). However, this interface loosely resembles the interaction of both S13 with RNA and the H2TH motif of endonuclease VIII with DNA (Figure 6B, E and F). The H2TH motifs of S13 and endonuclease VIII are, however, embedded within larger structures that make extensive

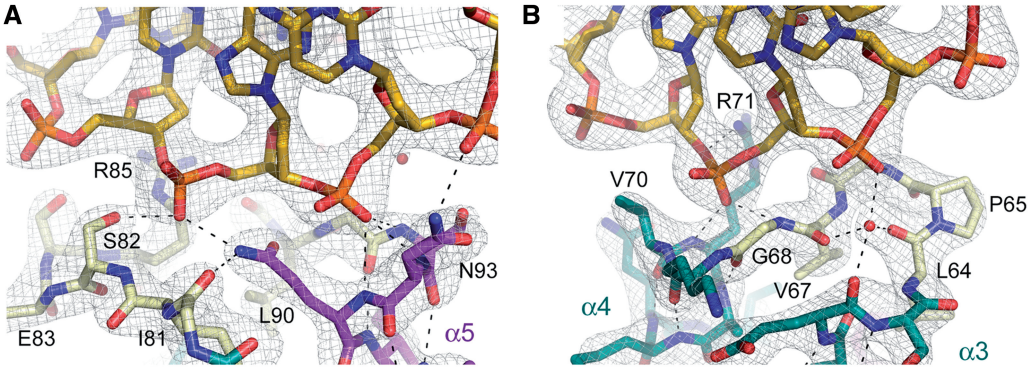

Figure 7. sIHF–DNA interaction. (**A**) Detail of the interaction between the H2TH lid and duplex I. The refined model is shown as colour-coded sticks and the 2Fo-Fc electron density map contoured at 1.0 σ. Hydrogen bonds are shown as dashed lines. (**B**) Detail of the interaction between the H2TH motif and duplex II. The refined model is shown as colour-coded sticks and the 2Fo-Fc electron density map contoured at 1.0 σ.

contacts with DNA or RNA molecules, and hence for these proteins, the DNA-binding role of the H2TH domain is predicted to be largely peripheral (54,56,57), with other protein domains ensuring proper DNA binding.

DISCUSSION

We have shown here that sIHF makes important contributions to *Streptomyces* development and secondary metabolism, but is dispensable for growth and viability. Loss of *sIHF* leads to defects in chromosome compaction, chromosome segregation, antibiotic production and spore septum placement. Collectively, our data strongly support a role for sIHF as a nucleoid-associated protein governing chromosome dynamics in *S. coelicolor*. This function is most evident during sporulation, which is the only time in the *Streptomyces* life cycle that chromosome compaction and segregation occur. While a number of classical nucleoid-associated proteins in *S. coelicolor* impact chromosome behaviour during sporulation, Δ*sIHF* mutants exhibit distinct phenotypic characteristics when compared with these other mutant strains. For example, the increased nucleoid size observed for the Δ*sIHF* mutant is a property shared with *smc* (58), *hupS* (59) and *dpsA* (60) mutants in *S. coelicolor*. These all encode classical nucleoid-associated proteins: SMC proteins play a pivotal role in the structural maintenance of chromosomes (61); HupS is one of two HU-like proteins encoded by *S. coelicolor* (59); and Dps-like proteins protect DNA from stressful conditions, in part through their ability to compact the chromosome (62). In a *hupS* mutant, chromosome condensation defects are coupled with reduced spore pigmentation and compromised spore dormancy, but the spores themselves are of uniform shape and size and contain appropriately segregated chromosomes (59), unlike those of the Δ*sIHF* mutant. Mutations in *smc* do not affect spore shape but lead to increased anucleate spores (58,63), equivalent to that observed here for the Δ*sIHF* mutants (~7–8%). The 'bilobed' chromosomal architecture occasionally observed for the Δ*sIHF* mutant was not shared with either *smc* or *hupS* mutants, but has been seen in *scpA* and *scpB* mutants (63), where these genes encode two accessory proteins required for SMC function (64). Finally, *dpsA* mutants exhibit variation in spore size and defects in chromosome condensation, like Δ*sIHF* mutants, but have wild-type levels of anucleate spores (60). It will be interesting to see whether there is any functional redundancy shared by sIHF and these diverse nucleoid-associated proteins.

Like many well-characterized nucleoid-associated proteins in *E. coli*, sIHF is a small, positively charged protein. It is, however, structurally unrelated to not only the archetypal IHF, HU and H-NS proteins but also to all known nucleoid-associated proteins. The sIHF structure has revealed that it binds DNA as a monomer, and that DNA binding encompasses 8 bp. It appears to have no obvious DNA-binding specificity, based on both our DNA-binding assays and the sIHF–DNA crystal structure. We cannot, however, exclude the possibility that higher affinity sIHF-binding sequences exist until a comprehensive binding screen is undertaken. For instance, IHF can associate with non-specific DNA sequences, although it recognizes a preferred sequence with ~1000-fold greater affinity (65). In binding DNA, sIHF interacts primarily with the phosphate backbone, but several positively charged residues interact with DNA through the minor groove—a feature shared with many architectural proteins including IHF- and HU-like proteins. sIHF does, however, lack an analogous proline residue found in every member of the HU/IHF family and, therefore, unlike these proteins, its binding does not lead to significant bending of the DNA (50). Indeed, the overall architecture and DNA-binding mechanism of sIHF are unrelated to other nucleoid-associated proteins, confirming that sIHF is not a homologue of IHF, and that it represents a new category of nucleoid-associated protein. The observation that sIHF has two potential DNA contact points suggests that it may have the capacity to bridge different DNA molecules, or stabilize (but not introduce) DNA bends. This differs from the DNA-bridging capabilities of H-NS and Lsr2, which bind single sites and bring disparately oriented DNA segments together through oligomerization.

Notably, other proteins with domains bearing structural similarity to the sIHF H2TH domain (endonuclease VIII, ribosomal protein S13 and topoisomerase VI) are all nucleic acid-binding proteins; however, for those whose structures have been solved in complex with either DNA (exonuclease VIII) or RNA (S13), their H2TH domains appear to contribute only peripherally to nucleic acid association (54,56,57). It is therefore possible that sIHF acts in conjunction with other proteins, perhaps through its extended N-terminal helix (residues 14–35 in the structure), as this helix does not contribute to DNA association, and yet is highly conserved. An intriguing interaction candidate would be the single type I topoisomerase (TopA) encoded by *S. coelicolor* and other actinobacteria, given that sIHF impacts DNA topology in a TopA-dependent manner in *in vitro* topoisomerase assays, and that the H2TH domain is also found in topoisomerase VI. It is worth noting, however, that topoisomerase VI is a type II topoisomerase (cleaves both DNA strands and changes the linking number by 2), while the *S. coelicolor* TopA is a type I enzyme (cleaves a single DNA strand and changes the linking number by 1), and thus these enzymes would act via different mechanisms.

IHF in *E. coli* functions to promote phage DNA integration, nucleoid compaction through its ability to bend DNA and gene regulation through its DNA-binding capabilities. While mIHF (the sIHF orthologue in mycobacteria) is required for phage integrase activity, it is unclear as to whether sIHF will have an equivalent role, as we found plasmid vectors bearing ϕC31-(pSET152/pIJ82) integration elements were readily incorporated into the chromosome of an Δ*sIHF* mutant. Interestingly, phage integrase activity often proceeds via a topoisomerase I-like mechanism (66), and as discussed above, we have shown here that sIHF has both functional and structural connections with topoisomerase enzymes. While TopA has not previously been implicated in chromosome dynamics during *Streptomyces* sporulation, investigations in other organisms have connected topoisomerase I with both plasmid and chromosome condensation/segregation (67–69). The striking effect of sIHF on TopA activity *in vitro* could provide a reasonable explanation for the reduced chromosome compaction observed for an *sIHF* mutant during sporulation. sIHF appears to promote supercoiling in a topoisomerase-dependent manner; if this accurately reflects its role *in vivo*, loss of sIHF would be expected to correlate with a more diffuse chromosome architecture.

In *E. coli,* many nucleoid-associated proteins also function as global transcription regulators. For example, IHF influences the expression of anywhere between 150 and 500 genes, while HU affects the expression (both positively and negatively) of >900 genes (70,71). Previous work (44) has suggested that sIHF may directly regulate antibiotic production in *S. coelicolor* by binding upstream of two pathway-specific regulatory genes: *redD* (which encodes a direct activator of undecylprodigiosin production) and *actII-orf4* (which encodes the direct activator of actinorhodin production). Our work supports an important role for sIHF in antibiotic biosynthesis, as an *sIHF* mutant was significantly impaired in its antibiotic production under the conditions we tested. We are not confident, however, that this effect is a direct one, as both our work, and work by Yang *et al.* (23), seem to suggest that sIHF can bind any DNA fragment ≥19 bp *in vitro*. Irrespective of direct or indirect sIHF association with antibiotic biosynthetic genes, it is obvious that the effect of sIHF on antibiotic production is not straightforward. Yang *et al.* (23) had previously reported enhanced actinorhodin and undecylprodigiosin production by their *sIHF* mutant under all growth conditions examined, including rich (glucose-containing) agar medium, and minimal agar medium supplemented with different carbon sources (glucose, chitin) and various amino acids. Consistent with these observations, we found actinorhodin production by the *sIHF* mutant was enhanced during growth on rich agar medium. We did, however, observe reduced antibiotic (actinorhodin and CDA) levels for the *sIHF* mutant relative to that of the wild-type strain, during growth on other solid media (soy flour with mannitol [MS] agar; nutrient agar), suggesting that the effect of sIHF on antibiotic production may be carbon source dependent. We also observed differences during liquid culture, where growth in a rich (glucose-based) liquid medium resulted in markedly reduced levels of both actinorhodin and undecylprodigiosin by the *sIHF* mutant, compared with its wild-type parent. Taken together, these results suggest that sIHF-mediated antibiotic effects are differentially responsive to media composition and growth conditions.

The diverse, but reproducible, phenotypic characteristics associated with *sIHF* mutation range from defects in antibiotic production, to aberrant sporulation, chromosome segregation and chromosome compaction. This suggests that sIHF nucleoid association and DNA binding likely impact gene expression on a global level, and this will be an exciting avenue to pursue in the future.

ACCESSION NUMBERS

Atomic coordinates and structure factors have been deposited with the Protein Data Bank (accession code 4ITQ).

SUPPLEMENTARY DATA

Supplementary Data are available at NAR Online: Supplementary Tables 1 and 2 and Supplementary Figures 1–5.

ACKNOWLEDGEMENTS

We would like to thank David Capstick and Hindra for critical reading of the article and for helpful suggestions.

FUNDING

McMaster University, a grant from the Canadian Institutes of Health Research [MOP-67189 to A.G.]; Canada Research Chairs (CRC) program (to M.A.E.)

and a graduate student award from NSERC (to J.P.S.). Funding for open access charges: McMaster University.

Conflict of interest statement. None declared.

REFERENCES

1. Dillon,S.C. and Dorman,C.J. (2010) Bacterial nucleoid-associated proteins, nucleoid structure and gene expression. *Nat. Rev. Microbiol.*, **8**, 185–195.
2. Browning,D.F., Grainger,D.C. and Busby,S.J.W. (2010) Effects of nucleoid-associated proteins on bacterial chromosome structure and gene expression. *Curr. Opin. Microbiol.*, **13**, 773–780.
3. Fang,F.C. and Rimsky,S. (2008) New insights into transcriptional regulation by H-NS. *Curr. Opin. Microbiol.*, **11**, 113–120.
4. Dame,R.T., Noom,M.C. and Wuite,G.J.L. (2006) Bacterial chromatin organization by H-NS protein unravelled using dual DNA manipulation. *Nature*, **444**, 387–390.
5. Guo,F. and Adhya,S. (2007) Spiral structure of *Escherichia coli* HUαβ provides foundation for DNA supercoiling. *Proc. Natl Acad. Sci. USA*, **104**, 4309–4314.
6. Swinger,K.K. and Rice,P.A. (2004) IHF and HU: flexible architects of bent DNA. *Curr. Opin. Struct. Biol.*, **14**, 28–35.
7. Gordon,B.R.G., Li,Y., Wang,L., Sintsova,A., van Bakel,H., Tian,S., Navarre,W.W., Xia,B. and Liu,J. (2010) Lsr2 is a nucleoid-associated protein that targets AT-rich sequences and virulence genes in *Mycobacterium tuberculosis*. *Proc. Natl Acad. Sci. USA*, **107**, 5154–5159.
8. Gordon,B.R.G., Imperial,R., Wang,L., Navarre,W.W. and Liu,J. (2008) Lsr2 of *Mycobacterium* represents a novel class of H-NS-like proteins. *J. Bacteriol.*, **190**, 7052–7059.
9. Pedulla,M.L., Lee,M.H., Lever,D.C. and Hatfull,G.F. (1996) A novel host factor for integration of mycobacteriophage L5. *Proc. Natl Acad. Sci. USA*, **93**, 15411–15416.
10. Pedulla,M.L. and Hatfull,G.F. (1998) Characterization of the *mIHF* gene of *Mycobacterium smegmatis*. *J. Bacteriol.*, **180**, 5473–5477.
11. Sassetti,C.M., Boyd,D.H. and Rubin,E.J. (2003) Genes required for mycobacterial growth defined by high density mutagenesis. *Mol. Microbiol.*, **48**, 77–84.
12. Bushman,W., Thompson,J.F., Vargas,L. and Landy,A. (1985) Control of directionality in lambda site specific recombination. *Science*, **230**, 906–911.
13. Ditto,M.D., Roberts,D. and Weisberg,R.A. (1994) Growth phase variation of integration host factor level in *Escherichia coli*. *J. Bacteriol.*, **176**, 3738–3748.
14. Lee,M.H. and Hatfull,G.F. (1993) Mycobacteriophage L5 integrase-mediated site-specific integration in vitro. *J. Bacteriol.*, **175**, 6836–6841.
15. Cole,S.T., Brosch,R., Parkhill,J., Garnier,T., Churcher,C., Harris,D., Gordon,S.V., Eiglmeier,K., Gas,S., Barry,C.E. *et al.* (1998) Deciphering the biology of *Mycobacterium tuberculosis* from the complete genome sequence. *Nature*, **393**, 537–544.
16. Bentley,S.D., Chater,K.F., Cerdeño-Tárraga,A.M., Challis,G.L., Thomson,N.R., James,K.D., Harries,D.E., Quail,M.A., Kieser,H., Harper,D. *et al.* (2002) Complete genome sequence of the model actinomycete *Streptomyces coelicolor* A3(2). *Nature*, **417**, 141–147.
17. Cerdeño-Tárraga,A.M., Efstratiou,A., Dover,L.G., Holden,M.T., Pallen,M., Bentley,S.D., Besra,G.S., Churcher,C., James,K.D., De Zoysa,A. *et al.* (2003) The complete genome sequence and analysis of *Corynebacterium diphtheriae* NCTC13129. *Nucleic Acids Res.*, **31**, 6516–6523.
18. Thanky,N.R., Young,D.B. and Robertson,B.D. (2007) Unusual features of the cell cycle in mycobacteria: polar-restricted growth and the snapping-model of cell division. *Tuberculosis*, **87**, 231–236.
19. Flärdh,K., Richards,D.M., Hempel,A.M., Howard,M. and Buttner,M.J. (2012) Regulation of apical growth and hyphal branching in *Streptomyces*. *Curr. Opin. Microbiol.*, **15**, 737–743.
20. Flärdh,K. and Buttner,M.J. (2009) *Streptomyces* morphogenetics: dissecting differentiation in a filamentous bacterium. *Nat. Rev. Microbiol.*, **7**, 36–49.
21. Hopwood,D.A. (2007) *Streptomyces in Nature and Medicine: The Antibiotic Makers*. Oxford University Press, Oxford, NY.
22. Champness,W.C. and Chater,K.F. (1994) Regulation and integration of antibiotic production and morphological differentiation in *Streptomyces* spp. In: Piggot,P., Moran,C.P. and Youngman,P. (eds), *Regulation of Bacterial Differentiation*. American Society for Microbiology, Washington, DC, pp. 61–94.
23. Yang,Y.H., Song,E., Willemse,J., Park,S.H., Kim,W.S., Kim,E.J., Lee,B.R., Kim,J.N., van Wezel,G.P. and Kim,B.G. (2012) A novel function of *Streptomyces* integration host factor (sIHF) in the control of antibiotic production and sporulation in *Streptomyces coelicolor*. *Antonie Van Leeuwenhoek*, **101**, 479–492.
24. Kieser,T., Bibb,M.J., Buttner,M.J., Chater,K.F. and Hopwood,D.A. (2000) *Practical Streptomyces Genetics*. The John Innes Foundation, Norwich, UK.
25. Chakraburtty,R. and Bibb,M.J. (1997) The ppGpp synthetase gene (*relA*) of *Streptomyces coelicolor* A3(2) plays a conditional role in antibiotic production and morphological differentiation. *J. Bacteriol.*, **179**, 5854–5861.
26. Paget,M.S., Chamberlin,L., Atrih,A., Foster,S.J. and Buttner,M.J. (1999) Evidence that the extracytoplasmic function sigma factor σ^E is required for normal cell wall structure in *Streptomyces coelicolor* A3(2). *J. Bacteriol.*, **181**, 204–211.
27. Gust,B., Challis,G.L., Fowler,K., Kieser,T. and Chater,K.F. (2003) PCR-targeted *Streptomyces* gene replacement identifies a protein domain needed for biosynthesis of the sesquiterpene soil odor geosmin. *Proc. Natl Acad. Sci. USA*, **100**, 1541–1546.
28. Datsenko,K.A. and Wanner,B.L. (2000) One-step inactivation of chromosomal genes in *Escherichia coli* K-12 using PCR products. *Proc. Natl Acad. Sci. USA*, **97**, 6640–6645.
29. Janssen,G.R. and Bibb,M.J. (1993) Derivatives of pUC18 that have *Bgl*II sites flanking a modified multiple cloning site and that retain the ability to identify recombinant clones by visual screening of *Escherichia coli* colonies. *Gene*, **124**, 133–134.
30. Sun,J., Kelemen,G.H., Fernández-Abalos,J.M. and Bibb,M.J. (1999) Green fluorescent protein as a reporter for spatial and temporal gene expression in *Streptomyces coelicolor* A3(2). *Microbiology*, **145**, 2221–2227.
31. Duong,A., Capstick,D.S., Di Berardo,C., Findlay,K.C., Hesketh,A., Hong,H.J. and Elliot,M.A. (2012) Aerial development in *Streptomyces coelicolor* requires sortase activity. *Mol. Microbiol.*, **83**, 992–1005.
32. Redenbach,M., Kieser,H.M., Denapaite,D., Eichner,A., Cullum,J., Kinashi,H. and Hopwood,D.A. (1996) A set of ordered cosmids and a detailed genetic and physical map for the 8 Mb *Streptomyces coelicolor* A3(2) chromosome. *Mol. Microbiol.*, **21**, 77–96.
33. Abramoff,M.D., Magalhaes,P.J. and Ram,S.J. (2004) Image processing with ImageJ. *Biophotonics Int.*, **11**, 33–42.
34. Haiser,H.J., Yousef,M.R. and Elliot,M.A. (2009) Cell wall hydrolases affect germination, vegetative growth, and sporulation in *Streptomyces coelicolor*. *J. Bacteriol.*, **191**, 6501–6512.
35. McKenzie,N.L. and Nodwell,J.R. (2007) Phosphorylated AbsA2 negatively regulates antibiotic production in *Streptomyces coelicolor* through interactions with pathway-specific regulatory gene promoters. *J. Bacteriol.*, **189**, 5284–5292.
36. Kang,S.G., Jin,W., Bibb,M. and Lee,K.J. (1998) Actinorhodin and undecylprodigiosin production in wild-type and *relA* mutant strains of *Streptomyces coelicolor* A3(2) grown in continuous culture. *FEMS Microbiol. Lett.*, **168**, 221–226.
37. Hindra, Pak,P. and Elliot,M.A. (2010) Regulation of a novel gene cluster involved in secondary metabolite production in *Streptomyces coelicolor*. *J. Bacteriol.*, **192**, 4973–4982.
38. Hendrickson,W.A., Horton,J.R. and LeMaster,D.M. (1990) Selenomethionyl proteins produced for analysis by multiwavelength anomalous diffraction (MAD): a vehicle for direct determination of three-dimensional structure. *EMBO J.*, **9**, 1665–1672.
39. Otwinowski,Z. and Minor,W. (1997) Processing of X-ray diffraction data. *Methods Enzymol.*, **276**, 307–326.
40. Terwilliger,T.C. and Berendzen,J. (1999) Automated MAD and MIR structure solution. *Acta. Crystallogr.*, **D55**, 849–861.
41. Afonine,P.V., Gross-Kunstleve,R.W., Echols,M., Headd,J.J., Moriarty,N.W., Mustyakimov,M., Terwilliger,T.C.,

Urzhumtsev,A., Zwart,P.H. and Adams,P.D. (2012) Towards automated crystallographic structure refinement with phenix.refine. *Acta Crystallogr. D Biol. Crystallogr*, **68**, 352–367.
42. Emsley,P. and Cowtan,K. (2004) Coot: model-building tools for molecular graphics. *Acta. Cryst.*, **D60**, 2126–2132.
43. Elliot,M.A., Karoonuthaisiri,N., Huang,J., Bibb,M.J., Cohen,S.N., Kao,C.M. and Buttner,M.J. (2003) The chaplins: a family of hydrophobic cell-surface proteins involved in aerial mycelium formation in *Streptomyces coelicolor*. *Genes Dev.*, **17**, 1727–1740.
44. Park,S.S., Yang,Y.H., Song,E., Kim,E.J., Kim,W.S., Sohng,J.K., Lee,H.C., Liou,K.K. and Kim,B.G. (2009) Mass spectrometric screening of transcriptional regulators involved in antibiotic biosynthesis in *Streptomyces coelicolor* A3(2). *J. Ind. Microbiol. Biotechnol.*, **36**, 1073–1083.
45. Elliot,M.A., Bibb,M.J., Buttner,M.J. and Leskiw,B.K. (2001) BldD is a direct regulator of key developmental genes in *Streptomyces coelicolor* A3 (2). *Mol. Microbiol.*, **40**, 257–269.
46. Owen-Hughes,T.A., Pavitt,G.D., Santos,D.S., Sidebotham,J.M., Hulton,C.S., Hinton,J.C.D. and Higgins,C.F. (1992) The chromatin-associated protein H-NS interacts with curved DNA to influence DNA topology and gene expression. *Cell*, **71**, 255–265.
47. Azam,T.A. and Ishihama,A. (1999) Twelve species of the nucleoid-associated protein from *Escherichia coli*. *J. Biol. Chem.*, **274**, 33105–33113.
48. Swinger,K.K. and Rice,P.A. (2007) Structure-based analysis of HU-DNA binding. *J. Mol. Biol.*, **365**, 1005–1016.
49. Hirano,M. and Hirano,T. (1998) ATP-dependent aggregation of single-stranded DNA by a bacterial SMC homodimer. *EMBO J.*, **17**, 7139–7148.
50. Rice,P.A., Yang,S., Mizuuchi,K. and Nash,H.A. (1996) Crystal structure of an IHF–DNA complex: a protein-induced DNA U-turn. *Cell*, **87**, 1295–1306.
51. Lorenz,M., Hillisch,A., Goodman,S.D. and Diekmann,S. (1999) Global structure similarities of intact and nicked DNA complexed with IHF measured in solution by fluorescence resonance energy transfer. *Nucleic Acids Res.*, **27**, 4619–4625.
52. Corbett,K.D. and Berger,J.M. (2003) Structure of the topoisomerase VI-B subunit: implications for type II topoisomerase mechanism and evolution. *EMBO J.*, **22**, 151–163.
53. Sugahara,M., Mikawa,T., Kumasaka,T., Yamamoto,M., Kato,R., Fukuyama,K., Inoue,Y. and Kuramitsu,S. (2000) Crystal structure of a repair enzyme of oxidatively damaged DNA, MutM (Fpg), from an extreme thermophile, *Thermus thermophilus* HB8. *EMBO J.*, **19**, 3857–3869.
54. Zharkov,D.O., Golan,G., Gilboa,R., Fernandes,A.S., Gerchman,S.E., Kycia,J.H., Rieger,R.A., Grollman,A.P. and Shoham,G. (2002) Structural analysis of an *Escherichia coli* endonuclease VIII covalent reaction intermediate. *EMBO J.*, **21**, 789–800.
55. Brodersen,D.E., Clemons,W.M., Carter,A.P., Wimberly,B.T. and Ramakrishnan,V. (2002) Crystal structure of the 30 S ribosomal subunit from *Thermus thermophilus*: structure of the proteins and their interactions with 16 S RNA. *J. Mol. Biol.*, **316**, 725–768.
56. Fromme,J.C. and Verdine,G.L. (2002) Structural insights into lesion recognition and repair by the bacterial 8-oxoguanine DNA glycosylase MutM. *Nat. Struct. Biol.*, **9**, 544–552.
57. Gilboa,R., Zharkov,D.O., Golan,G., Fernandes,A.S., Gerchman,S.E., Matz,E., Kycia,J.H., Grollman,A.P. and Shoham,G. (2002) Structure of formamidopyrimidine-DNA glycosylase covalently complexed to DNA. *J. Biol. Chem.*, **277**, 19811–19816.
58. Kois,A., Swiatek,M., Jakimowicz,D. and Zakrzewska-Czerwińska,J. (2009) SMC protein-dependent chromosome condensation during aerial hyphal development in *Streptomyces*. *J. Bacteriol.*, **191**, 310–319.
59. Salerno,P., Larsson,J., Bucca,G., Laing,E., Smith,C.P. and Flärdh,K. (2009) One of the two genes encoding nucleoid-associated HU proteins in *Streptomyces coelicolor* is developmentally regulated and specifically involved in spore maturation. *J. Bacteriol.*, **191**, 6489–6500.
60. Facey,P.D., Hitchings,M.D., Saavedra-Garcia,P., Fernandez-Martinez,L., Dyson,P.J. and Del Sol,R. (2009) *Streptomyces coelicolor* Dps-like proteins: differential dual roles in response to stress during vegetative growth and in nucleoid condensation during reproductive cell division. *Mol. Microbiol.*, **73**, 1186–1202.
61. Hirano,T. (2006) At the heart of the chromosome: SMC proteins in action. *Nat. Rev. Mol. Cell Biol.*, **7**, 311–322.
62. Nair,S. and Finkel,S.E. (2004) Dps protects cells against multiple stresses during stationary phase. *J. Bacteriol.*, **186**, 4192–4198.
63. Dedrick,R.M., Wildschutte,H. and McCormick,J.R. (2009) Genetic interactions of *smc*, *ftsK*, and *parB* genes in *Streptomyces coelicolor* and their developmental genome segregation phenotypes. *J. Bacteriol.*, **191**, 320–332.
64. Soppa,J., Kobayashi,K., Noirot-Gros,M.F., Oesterhelt,D., Ehrlich,S.D., Dervyn,E., Ogasawara,N. and Moriya,S. (2002) Discovery of two novel families of proteins that are proposed to interact with prokaryotic SMC proteins, and characterization of the *Bacillus subtilis* family members ScpA and ScpB. *Mol. Microbiol.*, **45**, 59–71.
65. Wang,S., Cosstick,R., Gardner,J.F. and Gumport,R.I. (1995) The specific binding of *Escherichia coli* integration host factor involves both major and minor grooves of DNA. *Biochemistry*, **34**, 13082–13090.
66. Kikuchi,Y. and Nash,H.A. (1979) Nicking-closing activity associated with bacteriophage lambda *int* gene product. *Proc. Natl Acad. Sci. USA*, **76**, 3760–3764.
67. Zhu,Q., Pongpech,P. and DiGate,R.J. (2001) Type I topoisomerase activity is required for proper chromosomal segregation in *Escherichia coli*. *Proc. Natl Acad. Sci. USA*, **98**, 9766–9771.
68. Minden,J.S. and Marians,K.J. (1986) *Escherichia coli* topoisomerase I can segregate replicating pBR322 daughter DNA molecules in vitro. *J. Biol. Chem.*, **261**, 11906–11917.
69. Wang,J.C. (2002) Cellular roles of DNA topoisomerases: a molecular perspective. *Nat. Rev. Mol. Cell Biol.*, **3**, 430–440.
70. Gama-Castro,S., Jiménez-Jacinto,V., Peralta-Gil,M., Santos-Zavaleta,A., Peñaloza-Spinola,M.I., Contreras-Moreira,B., Segura-Salazar,J., Muñiz-Rascado,L., Martínez-Flores,I., Salgado,H. *et al.* (2008) RegulonDB (version 6.0): gene regulation model of *Escherichia coli* K-12 beyond transcription, active (experimental) annotated promoters and Textpresso navigation. *Nucleic Acids Res.*, **36**, D120–D124.
71. Prieto,A.I., Kahramanoglou,C., Ali,R.M., Fraser,G.M., Seshasayee,A.S.N. and Luscombe,N.M. (2012) Genomic analysis of DNA binding and gene regulation by homologous nucleoid-associated proteins IHF and HU in *Escherichia coli* K12. *Nucleic Acids Res.*, **40**, 3524–3537.